

Incorporating Locality of Images to Generate Targeted Transferable Adversarial Examples

Zhipeng Wei^{1,2}, Jingjing Chen^{1,2†}, Zuxuan Wu^{1,2}, Yu-Gang Jiang^{1,2}

¹Shanghai Key Lab of Intelligent Information Processing, School of Computer Science, Fudan University

²Shanghai Collaborative Innovation Center on Intelligent Visual Computing
zpwei21@m.fudan.edu.cn, {chenjingjing, zxwu, ygj}@fudan.edu.cn

Abstract

Despite that leveraging the transferability of adversarial examples can attain a fairly high attack success rate for non-targeted attacks, it does not work well in targeted attacks since the gradient directions from a source image to a targeted class are usually different in different DNNs. To increase the transferability of target attacks, recent studies make efforts in aligning the feature of the generated adversarial example with the feature distributions of the targeted class learned from an auxiliary network or a generative adversarial network. However, these works assume that the training dataset is available and require a lot of time to train networks, which makes it hard to apply to real-world scenarios. In this paper, we revisit adversarial examples with targeted transferability from the perspective of universality and find that highly universal adversarial perturbations tend to be more transferable. Based on this observation, we propose the Locality of Images (LI) attack to improve targeted transferability. Specifically, instead of using the classification loss only, LI introduces a feature similarity loss between intermediate features from adversarial perturbed original images and randomly cropped images, which makes the features from adversarial perturbations to be more dominant than that of benign images, hence improving targeted transferability. Through incorporating locality of images into optimizing perturbations, the LI attack emphasizes that targeted perturbations should be universal to diverse input patterns, even local image patches. Extensive experiments demonstrate that LI can achieve high success rates for transfer-based targeted attacks. On attacking the ImageNet-compatible dataset, LI yields an improvement of 12% compared with existing state-of-the-art methods.

Introduction

Deep neural networks (DNNs) have been demonstrated to be susceptible to adversarial examples (Goodfellow, Shlens, and Szegedy 2014; Biggio et al. 2013), which are generated by adding small human-crafted perturbations that may lead to wrong prediction of DNNs. The existence of adversarial examples has raised serious security threats for DNNs. Even when the adversary has no access to the architecture and parameters of the attacked model, they can utilize adversarial examples generated from a surrogate white-box model to attack the black-box model, which is also known as cross-model transferability of adversarial examples. Such cross-

model adversarial transferability further makes a threat to DNN applications.

Recent studies (Dong et al. 2018; Xie et al. 2019; Wei et al. 2022a,b) have shown that the non-targeted adversarial transferability has attained high performance even when attacking robust trained models, as decision boundaries around one source image align well among different models. In contrast, the targeted adversarial transferability is more challenging due to the different gradient directions from one source image to the targeted class among models (Liu et al. 2017). The study of targeted adversarial transferability has become an important aspect of understanding inner-workings of DNNs.

Previous researches in this field have been devoted to training class-specific auxiliary networks (Inkawhich et al. 2020b,a) or generative adversarial networks (GANs) (Naseer et al. 2021), in order to learn feature distributions of the targeted class. Then the generated adversarial examples are optimized to match the learned feature distributions of the targeted class. Despite these methods have been demonstrated to be effective in improving the adversarial transferability towards targeted attacks, they usually suffer from poor usability in the real world, due to the data dependency and time-consuming training. On the contrary, non-targeted transferable attack methods that based on the Iterative Fast Gradient Sign Method (I-FGSM) (Kurakin, Goodfellow, and Bengio 2018) are more efficient, since they only depend on a single image and a surrogate white-box model. However, these methods do not work well in targeted attack scenarios. The Logit attack (Zhao, Liu, and Larson 2021) attributes this phenomenon to the attack unconvergence caused by a small number of iterations. Moreover, it shows that the combination of Diverse Input (DI) (Xie et al. 2019), Momentum Iterative (MI) (Dong et al. 2018) and Translation-invariant (TI) (Dong et al. 2019) with a large number of iterations, which are originally proposed in non-targeted attacks, can yield good results in targeted attacks. Hence, these malicious perturbations generated by smoothed and stabilized gradients in TI and MI lead to misclassifying diverse input patterns from DI. In other words, these perturbations are universal to different input patterns, which motivates us to investigate the universality of targeted perturbations.

Based on the above analysis, we conduct toy experiments to analyze the correlations between the universality of adver-

[†]Correspondence to: Jingjing Chen.

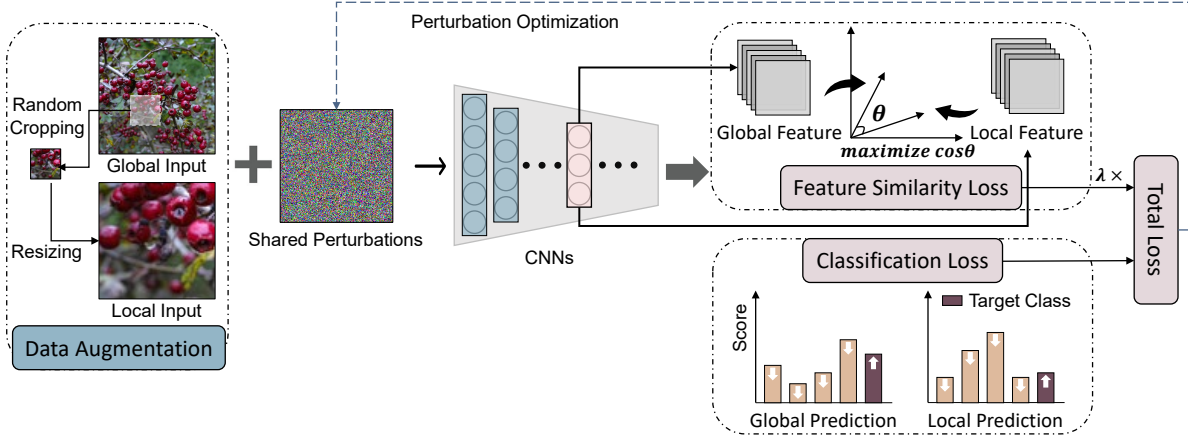


Figure 1: Overview of the proposed LI attack. The random cropping is applied to the given benign image to generate the local image patch. After cropping, the local patch is resized to the shape of the benign image. Then both benign and local adversarial images with the shared perturbations are input to a surrogate white-box CNN model. Finally, the gradients obtained from the classification loss and the feature similarity loss are used to optimize perturbations.

serial perturbations and the success rate of targeted attacks. Through the experiment, we discover that highly universal adversarial perturbations tend to be more transferable for target attacks. Moreover, we also find that the adversarial features tend to be more dominant than benign image features, which is consistent with the conclusion presented in (Zhang et al. 2020).

Based on these observations, we propose to create more diverse input patterns and increase the dominance of adversarial perturbations for the purpose of enhancing universality. More specifically, we introduce the Locality of Image (LI) attack, which applies random cropping to the input images and maximizes the cosine similarity of adversarial intermediate features between original images and local patches. Compared to input patterns used in DI (random resizing and padding), the locality of images focus on local structures of images. Through incorporating local structures into optimizing perturbations, LI generates adversarial perturbations that can be well generalized to both global and local structures. Besides, aligning adversarial intermediate features between global and local images aims to generate perturbations with high dominant features regardless of the superimposed images, hence enhancing targeted transferability.

Figure 1 gives an overview of the proposed LI attack. LI firstly applies the random cropping on benign images to obtain local cropped patches. Then it resizes local patches to the same shape with benign images. Consequently, global and local inputs with the shared perturbations are input to the white-box model. Finally, adversarial perturbations are updated by minimizing the classification loss (*e.g.*, Cross Entropy) between inputs and the targeted class and maximizing the feature similarity loss (*e.g.*, Cosine Similarity) of adversarial intermediate features between local and global inputs. Benefited from satisfying the prediction of the target class between global and local inputs and approximating adversarial intermediate features between the two, the proposed

locality of images and the feature similarity loss yield more universal perturbations to the diverse inputs of one specified image, thereby improving the cross-model targeted transferability. We briefly summarize our primary contributions as follows:

- We provide new insight into targeted transferability and investigate the universal property of targeted transferable perturbations. We observe that targeted transferable adversarial perturbations are more universal to other inputs and have more dominant features.
- The above observations motivate us to incorporate locality of images into optimizing perturbations for creating more diverse input patterns. Besides, we introduce a feature similarity loss between global and local adversarial features to generate targeted perturbations with dominant features, hence improving targeted transferability.
- We conduct comprehensive experiments to demonstrate that the proposed locality of images and the feature similarity loss can improve the cross-model targeted transferability of adversarial images. Besides, the proposed LI attack can be easily combined with existing methods.

Related Work

In this section, we review existing works on non-targeted transferable attacks as well as targeted transferable attacks.

Non-targeted Transferable Attacks

Non-targeted transferable attacks are based on the Iterative-Fast Gradient Sign Method (I-FGSM) (Kurakin, Goodfellow, and Bengio 2018), which iteratively calculates the gradient of the classification loss with respect to the input and update perturbations along the direction of maximizing the loss. The multiple-step update of I-FGSM leads to a high wrong prediction of white-box models. However, the generated adversarial examples are hard to attack other black-box models. This phenomenon is called over-fitting

to the white-box model (Kurakin, Goodfellow, and Bengio 2017). Subsequently, several works perform data augmentation or advanced gradient calculation to overcome the over-fitting problem. Data augmentation creates various input patterns, which generate adversarial perturbations with a generic pattern. For the input images, Diverse Input (DI) (Xie et al. 2019) performs random resizing and padding, Scale-invariant method (SIM) (Lin et al. 2020) applies scale transformation. However, these data augmentation approaches neglect to consider more diverse input patterns (*e.g.*, random cropping in this paper), and focus on the loss-preserving transformation (Lin et al. 2020). This is because the gradient direction fluctuates violently under more diverse input patterns for non-target attacks without specified target classes. Advanced gradient calculation pays attention to changing gradient calculation methods or designing a new loss function. For changing gradient calculation, the momentum term (Dong et al. 2018) and the Nesterov accelerated gradient (Lin et al. 2020) can be incorporated with I-FGSM to stabilize gradients. Translation-Invariant (TI) (Dong et al. 2019) smooths gradients through a pre-defined convolution kernel in order to mitigate the over-fitting problem. Skip Gradient Method (SGM) (Wu et al. 2020a) modifies the path of gradient backpropagation by skipping residual modules. Variance Tuning (Wang and He 2021) utilizes gradients from data points around previous data to avoid over-fitting. For designing a new loss function, Attention-guided Transfer Attack (ATA) (Wu et al. 2020b) and Feature Importance-aware Attack (FIA) (Wang et al. 2021) disrupt important features that are likely to be utilized in other black-box models. ATA applies Grad-CAM (Selvaraju et al. 2017) to represent attention weights of features. Different to ATA, FIA computes averaged gradients of features among various augmented inputs as attention weights. However, these new loss functions are restricted to global structures. In contrast, this paper calculates the feature similarity loss between global and local structures of images.

Targeted Transferable Attacks

The targeted transferable attacks are more challenging than the non-targeted transferable attacks due to the specified target class. One way is to train auxiliary networks for capturing feature distributions of the targeted class. Feature Distribution Attack (FDA) (Inkawhich et al. 2020b) utilizes the intermediate features of the training dataset from the white-box model to train a binary classifier, which predicts the probability that the current feature belongs to the targeted class. Then, Through learning class-wise and layer-wise feature distributions, FDA generates targeted transferable adversarial perturbations by maximizing the probability outputted from the trained binary classifier. Subsequently, $FDA^N + xent$ (Inkawhich et al. 2020a) incorporates the CE loss and multi-layer information with FDA, achieving better performance. Transferable targeted perturbations (TTP) (Naseer et al. 2021) trains a generator to synthesize perturbations that seek to have similar features with targeted samples in the latent space of a pretrained discriminator. This series of FDA works and TTP improve the performance of targeted transferable attacks, but require training auxiliary

networks with the training dataset. To improve the efficiency of targeted transferable attacks, another way is based on I-FGSM. Activation Attack (AA) (Inkawhich et al. 2019) replace the classification loss with a euclidean distance loss between features of adversarial and targeted images. However, AA depends on the selected examples of the targeted class and achieves low performance on the large resolution image dataset (*e.g.* ImageNet (Deng et al. 2009)). Different to AA, Po+Trip (Li et al. 2020) utilizes Poincaré distance metric to solve the noise curing. They also design a triplet loss for driving adversarial examples away from the original class. However, Po+Trip evaluates the attack performance only on easy transfer scenarios, and also achieves poor performance on the targeted scenario used in the Logit attack (Zhao, Liu, and Larson 2021). Logit (Zhao, Liu, and Larson 2021) attributes the poor performance of I-FGSM based methods to the restricted number of iterations. Thus, Logit enlarges the number of iterations for ensuring the convergence of attacks. In addition, to overcome the gradient vanishment caused by the large iterations, Logit utilizes gradients of the targeted logit output with respect to inputs to update perturbations. Different to them, our method leverages the global and local structures to generate adversarial examples with high universality, hence improving targeted transferability. Note that the proposed LI methods can be easily combined with existing methods.

Methodology

Preliminary

Let f represent the white-box surrogate model, v be the black-box victim model, $x \in \mathcal{X} \subset \mathbf{R}^{H \times W \times C}$ be the benign image with the ground-truth label $y \in \mathcal{Y} = \{1, 2, \dots, K\}$, where f and v are trained with the same training dataset, H , W , C denote the number of height, width and channels respectively, K is the number of classes. We use $f(x)$, $v(x)$ to be the prediction over the set of classes \mathcal{Y} . Given a specified targeted class y_t , the targeted transferable attacks aim to generate adversarial examples x_{adv} from the white-box model f that satisfy $v(x_{adv}) = y_t$. Following previous works, we enforce an L_∞ -norm constraint on perturbations, which can be formulated as $\|x_{adv} - x\|_\infty = \|\delta\|_\infty \leq \epsilon$, where δ is the perturbation, ϵ denotes a constant of the norm constraint. Given a classification loss J (*e.g.* CE loss) of f , the targeted attack of I-FGSM can be formulated as:

$$\delta_0 = 0, g_0 = 0, \quad (1)$$

$$g_{i+1} = \nabla_{\delta} J(f(x + \delta_i), y_t), \quad (2)$$

$$\delta_{i+1} = \delta_i - \alpha * \text{sign}(g_{i+1}), \quad (3)$$

$$\delta_{i+1} = \text{Clip}_{x, \epsilon}(\delta_{i+1}), \quad (4)$$

where δ_i , g_i denotes the adversarial perturbation and the gradient of the i -th iteration, $i = [0, \dots, I - 1]$, and I is the maximum number of iterations, α is the step size, the function $\text{Clip}_{x, \epsilon}(\cdot)$ projects δ to the vicinity of x for satisfying the L_∞ -norm constraint. Specifically, I-FGSM first initializes δ_0 and g_0 by 0 (Eq.1), then calculates the gradients of the loss function with respect to the perturbation (Eq.2), and drives the prediction of f on the adversarial example

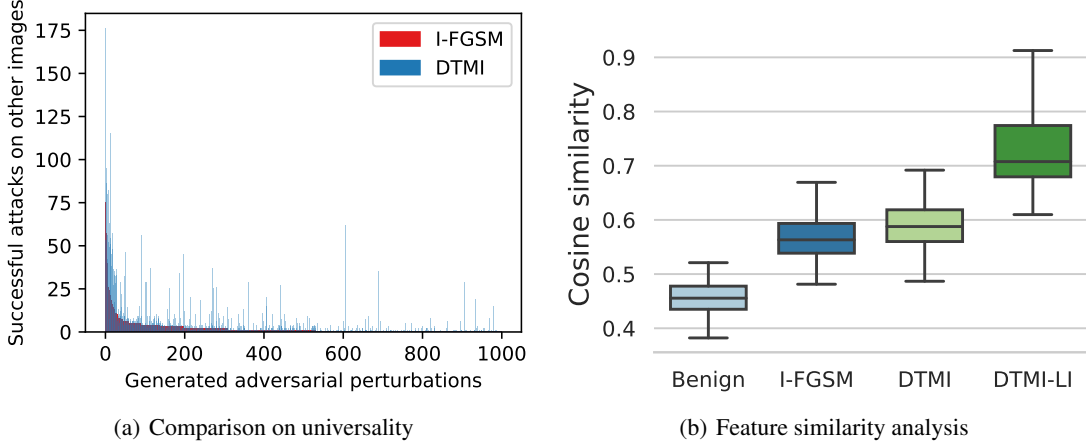


Figure 2: (a) For each targeted perturbation generated by I-FGSM or DTMI, we calculate the number of successful targeted attacks caused by adding this perturbation to benign images other than the original optimized image. (b) We average cosine similarity of intermediate features among different benign images or adversarial examples that are generated by adding the same perturbation to these benign images.

towards the targeted class by minimizing $J(f(x + \delta_i), y_t)$ (Eq.3), finally restricts the adversarial perturbation with the L_∞ -norm constraint (Eq.4). Eq.2, 3, 4 are performed alternately until the maximum iterations is reached. Through this greedy update, I-FGSM is easily caught in local maxima and over-fitting to f , which results in performing poorly for both non-targeted and targeted attacks. Therefore, Logit (Zhao, Liu, and Larson 2021) utilizes the combination of DI (Xie et al. 2019), TI (Dong et al. 2019) and MI (Dong et al. 2018) as the baseline, which achieves substantial performance in targeted transferable attacks with large numbers of iterations, rather than I-FGSM. For convenience, we abbreviate the name of this combination as DTMI. DTMI replaces Eq.2 with

$$g_{i+1} = \mu \cdot g_i + \frac{W \cdot \nabla_\delta J(f(T(x + \delta_i, p)), y_t)}{\|W \cdot \nabla_\delta J(f(T(x + \delta_i, p)), y_t)\|_1}, \quad (5)$$

where $T(x + \delta_i, p)$ perform random resizing and padding with a probability p in DI, W is the convolution kernel in TI, μ is a decay factor in MI. Following them, we incorporate the locality of images and the feature similarity loss with DTMI in order to boost targeted transferability.

Universality of Targeted Perturbations

Targeted transferable attacks aim to generate cross-model perturbations that drive the prediction of different models towards the same specified class. It requires that perturbations generated from one white-box model are model-agnostic or universal to different models. A simple way to meet this requirement is to optimize perturbations on ensemble models. However, it may be unsuitable in the real world, because the number of white-box models is limited. Intuitively, image-agnostic perturbations, which are highly dominant features than benign images (Zhang et al. 2020), may activate channels of different models with a high probability, hence becoming more universal to models. However, generating image-agnostic perturbations like (Moosavi-Dezfooli

et al. 2017) requires additional images for perturbation optimization and hence consumes more computation. On the contrary, DTMI can generate high targeted transferable perturbations without additional things, which motivates us to further investigate the universality of perturbations generated by DTMI.

A toy experiment is conducted to understand the correlation between universality and targeted transferability. We optimize perturbations on the ImageNet-compatible dataset (dataset details are in Section “Experimental Settings”) by I-FGSM and DTMI with the white-box model DenseNet121. For each image, the generated adversarial perturbation is then added to other images rather than itself to calculate the number of successful targeted attacks on DenseNet121. The classification loss is set as the CE loss.

The results are shown in Figure 2(a). The perturbations are sorted in descending order based on the number of successful attacks on other images for I-FGSM. As can be seen, the targeted perturbations tend to be universal to different images, even for the perturbations generated from I-FGSM. Besides, the diverse input patterns and advanced gradient calculation used in DTMI drive targeted transferable perturbations towards high generality, despite the fact that DTMI optimizes perturbations on one image. It experimentally demonstrates that targeted perturbations are generic to different images, which indicates that the generated targeted perturbations represent the feature distributions of targeted classes in the white-box model (DenseNet121), and even more dominant than benign images’ features.

To further illustrate the dominance of targeted perturbations, we calculate the averaged cosine similarity of intermediate features between images, which consist of benign images and adversarial images that are generated by adding each perturbation that can lead to the targeted prediction. The results are summarized in Figure 2(b). It can be observed that the features of adversarial images that are added

to the same perturbation become more similar. This suggests that, compared to benign images, targeted perturbations are the dominant feature.

These two experiments jointly show that DTMI leverages the targeted feature distributions of the white-box model to generate targeted perturbations with high dominant features, and improves the generality of perturbations by creating diverse inputs and stable gradient calculation. These factors motivate us to generate intra-image-agnostic perturbations by creating more diverse input patterns and improving the dominance of adversarial features for boosting cross-model targeted transferability.

Locality of Images (LI) Attack

Based on the analysis above, we propose to incorporate the Locality of Images into the iterative attacks, named LI. To create more diverse input patterns, we consider the random cropping, which crops images into a local image patch by the scale parameter $s = \{s_l, s_{int}\}$. Where s_l denotes the lower bound for the area of the random cropped images, and s_{int} is the interval value between the lower and upper bounds, thus $s_l + s_{int}$ is the upper bound. After cropping images, we resize them to the same shape with benign images. Let $Loc(x, s)$ be the random cropping and the resizing operations¹. In addition, to generate high universal perturbations, we propose a feature similarity loss to maximize the cosine similarity of intermediate features between the adversarial global and local inputs. It can be formulated by $CS(f_l(x + \delta_i), f_l(Loc(x, s) + \delta_i))$, where $f_l(\cdot)$ means to extract features from the l -th layer of the white-box model f , the function $CS(\cdot, \cdot)$ calculates cosine similarity score of features between adversarial global and local inputs. In summary, the proposed LI replaces Eq.2 with:

$$g_{i+1} = \nabla_{\delta} (J(f(x + \delta_i), y_t) + J(f(Loc(x, s) + \delta_i), y_t) - \lambda \cdot CS(f_l(x + \delta_i), f_l(Loc(x, s) + \delta_i))), \quad (6)$$

where λ weights the contribution of the classification loss and the proposed similarity loss.

In this way, the perturbation optimization in LI can leverage global and local structures of the inputs to improve the generalization of perturbations, and the maximization of the cosine similarity can align intermediate features between adversarial global and local inputs for improving the dominance of feature representation of perturbations. Following (Zhao, Liu, and Larson 2021), we integrate LI with DTMI, named DTMI-LI, which is illustrated in Algorithm 1. In the end, LI can generate adversarial perturbations with dominant features by incorporating locality of images, as shown in Figure 2(b), hence improving targeted transferability.

Experiment

Experimental Settings

Dataset and models Following (Zhao, Liu, and Larson 2021), we attack four diverse classifier architectures:

¹We perform it by RandomResizedCrop in torchvision and ignore the parameter of the random aspect ratio.

Algorithm 1: DTMI-LI attack

Input: the classification loss function J , white-box model f , benign image x , targeted class y_t .
Parameter: The perturbation budget ϵ , iteration number I , step size α , scale parameter $s = \{s_l, s_{int}\}$, weighted parameter λ , and DTMI parameters $T(\cdot, p)$, W , μ .
Output: The adversarial example x_{adv} .

```

1: Initialize  $\delta_0$  and  $g_0$  by Eq.1
2: for  $i = 0$  to  $I - 1$  do
3:    $g_{i+1} = \nabla_{\delta} (J(f(T(x + \delta_i, p)), y_t) + J(f(T(Loc(x, s) + \delta_i), p), y_t) - \lambda \cdot CS(f_l(T(x + \delta_i, p)), f_l(T(Loc(x, s) + \delta, p))))$ 
4:    $g_{i+1} = \mu \cdot g_i + \frac{W \cdot g_{i+1}}{\|W \cdot g_{i+1}\|_1}$ 
5:   Update and Clip  $\delta_{i+1}$  by Eq.3, 4
6: end for
7: return  $x + \delta_I$ 

```

Model	Layer 1	Layer 2	Layer 3	Layer 4
Res50	Block-1	Block-2	Block-3	Block-4
Den121	Block-1	Block-2	Block-3	Block-4
VGG16	ReLU-4	ReLU-7	ReLU-10	ReLU-13
Inc-v3	Conv-4a	Mix-5d	Mix-6e	Mix-7c

Table 1: Intermediate layers for feature extraction. “Block” means the basic block in ResNet50 and DenseNet121. “ReLU-k” denotes the k -th ReLU layer.

ResNet50 (He et al. 2016), DenseNet121 (Huang, Liu, and Weinberger 2017), VGGNet16 (Simonyan and Zisserman 2015), and Inception-v3 (Szegedy et al. 2016) with the ImageNet-compatible dataset². The architectures of these four models are more diverse and challenging than the ones used in (Li et al. 2020). The used dataset is firstly introduced by the NIPS 2017 Competition on Adversarial Attacks and Defenses. It consists of 1,000 images and corresponding labels for targeted adversarial attacks.

Attack setting We use the Targeted Attack Success Rate (TASR) to evaluate the targeted attack on one black-box model, which is the rate of adversarial examples that are successfully classified as the targeted class by the black-box model. Hence, the methods with higher TASR can generate adversarial examples with high targeted transferability. Following (Zhao, Liu, and Larson 2021), we set the maximum perturbation as $\epsilon = 16$, the step size as $\alpha = 2$, the maximum number of iterations as $I = 300$, DTMI with the original parameters as the baseline attack. For each model, we select layer 1/2/3/4 from bottom to top layer (as shown in Table 1) to calculate the feature similarity loss.

²https://github.com/cleverhans-lab/cleverhans/tree/master/cleverhans_v3.1.0/examples/nips17_adversarial_competition/dataset

Attack	White-box Model: Res50			White-box Model: Dense121		
	→ Dense121	→ VGG16	→ Inc-v3	→ Res50	→ VGG16	→ Inc-v3
DTMI-CE	27.1/39.7/44.3	18.9/27.6/29.4	2.2/3.4/4.1	12.9/16.7/18.4	8.1/10.6/10.6	1.7/2.2/3.2
DTMI-CE-LI	6.3/28.1/ 51.7	3.1/21.4/ 41.6	0.6/5.2/ 8.9	2.3/18.2/ 33.0	1.1/14.6/ 28.9	0.3/5.5/ 10.9
DTMI-Logit	30.4/64.4/71.8	22.6/55.1/62.8	2.7/7.1/9.6	16.1/39.3/43.7	13.5/33.0/38.1	2.1/7.1/7.7
DTMI-Logit-LI	23.7/64.8/ 75.1	16.9/56.8/ 67.7	1.8/7.7/ 11.2	12.7/42.2/ 50.0	9.5/37.3/ 45.1	1.7/7.9/ 10.3
Attack	White-box Model: VGG16			White-box Model: Inc-v3		
	→ Res50	→ Dense121	→ Inc-v3	→ Res50	→ Dense121	→ VGG16
DTMI-CE	0.6/0.6/0.5	0.4/0.3/0.4	0.0/0.0/0.0	0.8/1.8/2.4	0.8/2.4/2.9	0.7/1.3/1.8
DTMI-CE-LI	0.2/1.6/ 1.8	0.3/1.5/ 1.6	0.0/0.2/ 0.1	0.4/1.6/ 2.9	0.2/1.8/ 4.6	0.0/1.2/ 2.2
DTMI-Logit	3.0/9.6/11.3	3.2/12.0/13.7	0.1/0.6/0.7	0.9/2.0/2.8	1.1/3.3/5.0	0.6/2.2/ 3.9
DTMI-Logit-LI	2.7/12.3/ 13.2	3.6/13.4/ 15.3	0.1/1.1/ 0.8	0.8/2.7/ 4.3	1.1/3.9/ 7.2	0.5/2.2/ 3.9

Table 2: TASR of all black-box models under four attack scenarios using ResNet50, DenseNet121, VGGNet16 and Inception-v3 as white-box models, respectively. We conduct these experiments three times and report TASR with 20/100/300 iterations. The best results with 300 iterations are in bold.

Ensemble Attack	Black-box Model				Average
	Res50	Dense121	VGG16	Inc-v3	
DTMI-CE	31.1	55.2	51.6	16.1	38.5
DTMI-CE-LI	42.8	55.2	67.9	24.2	47.5
DTMI-Logit	70.2	82.3	82.2	29.1	65.9
DTMI-Logit-LI	75.9	83.0	84.1	35.4	69.6

Table 3: TASR of one black-box model in ensemble transfer attacks. TASR with 300 iterations is reported. The best results are in bold.

Performance Comparison

In this section, we integrate our method with several baselines: CE loss with DTMI (DTMI-CE) and Logit loss (Zhao, Liu, and Larson 2021) with DTMI (DTMI-Logit). We ignore Po+Trip (Li et al. 2020) because it has a lower performance than Logit loss. For LI, the weighted parameter λ is set as 0.4, the scale parameters s is set as (0.1, 0), and the layer 3 is used to extract features. These parameters will be discussed in Section “Ablation Studies”.

Single-model transferable attacks We conduct single-model transferable experiments by selecting one model as the white-box model to attack the other three black-box models. Table 2 shows the results. We have the following observations. First, the proposed LI method achieves higher TASR than DTMI-CE and DTMI-Logit by a large margin in almost all cases. It suggests that the proposed LI is suitable for different classification loss functions. Second, the attacks using ResNet50 and DenseNet121 as white-box models outperform that using VGGNet16 and Inception-v3, which is also observed in (Inkawich et al. 2019, 2020b; Zhao, Liu, and Larson 2021). It may be caused by the skip connection structure, which mitigates the gradient vanishing/exploding problem in a large number of iterations and emphasizes on features of lower layers by backpropagating gradients on both residual modules and skip connections. These features

tend to transfer among different models (Wu et al. 2020a; Wei et al. 2022b). Third, LI performs worse than other methods when using a small number of iterations (*e.g.* $I = 20$). This is because the local input pattern and the feature similarity loss require a large iteration for convergence.

Ensemble model transferable attacks As mentioned above, the targeted perturbations generated from a set of models are more model-agnostic, thus can obtain high cross-model transferability. Hence, we select one black-box model to attack, and use the other three models as white-box models. Following (Zhao, Liu, and Larson 2021), we simply assign equal weights to all white-box models. Results are shown in Table 3. As can be seen, compared to single-model transferable attacks, ensemble attacks achieve much better performance. It demonstrates that the model-agnostic perturbations can easily transfer to attack other models. In addition, the proposed LI further boosts the cross-model targeted transferability. However, the improvement of TASR gained from DTMI-Logit-LI is not so significant. This can be explained by the fact that the loss function value of Logit increases infinitely, while the value of cosine similarity is bounded. Thus, it impedes the maximization of feature similarity. Nevertheless, methods that are combined with LI can promote targeted transferability in all cases.

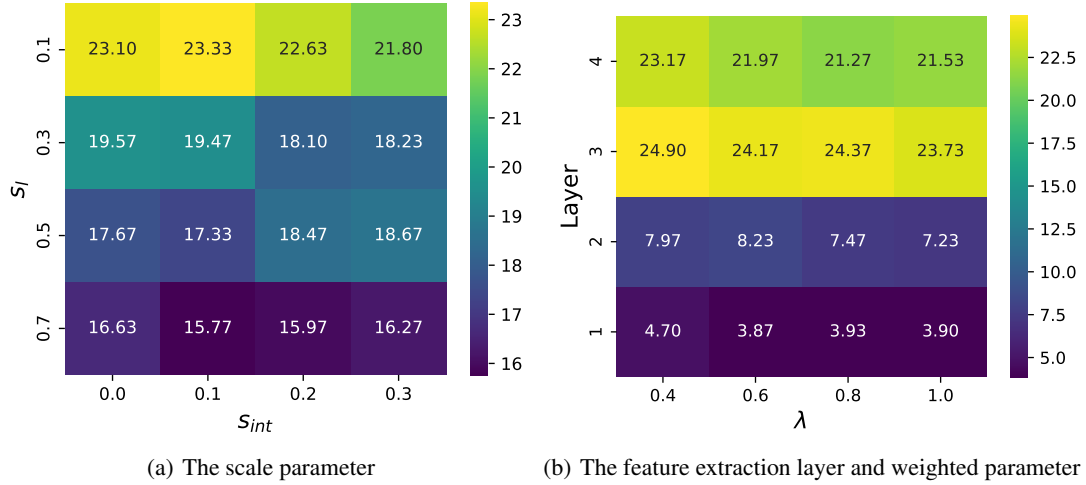


Figure 3: Average TASR with different values of hyperparameters in the attack.

Locality	Feature Similarity Loss	Averaged TASR
-	-	9.8
✓	-	10.9
✓	✓	15.6

Table 4: Average TASR (%) of black-box models for our proposed method with different component combinations. The classification loss is set as CE. ‘✓’ indicates that the component is used while ‘-’ indicates that it is not used. TASR is averaged among four attack scenarios using ResNet50, DenseNet121, VGGNet16 and Inceptionv3 as white-box models, respectively.

Ablation Studies

In this section, we investigate the effects of each component and various hyperparameters.

Effect of Components The evaluations are conducted on four attack scenarios using ResNet50, DenseNet121, VGGNet16 and Inceptionv3 as white-box models, respectively. We split LI into the locality of images and the feature similarity loss. Table 4 show the results of different component combinations. As can be seen, both components improve targeted transferability. And the improvement of TASR gained from feature similarity loss is more significant. Combining all components increases the average TASR by 59.18%. It demonstrates the effectiveness of each component in the proposed LI attack.

Effect of hyperparameters The evaluations are conducted by using densenet121 as the white-box model and averaging TASR among black-box models. The scale parameter s determines the area of cropped images. When the area is large, LI overlooks the local structure of inputs. Thus, it is vital to study optimal values of s . We fix the weighted parameter $\lambda = 1.0$, and the feature extraction layer as layer 3 due to the high transferability of mid-

dle layers (Wei et al. 2022b). Figure 3(a) shows the results with $s_l \in [0.1, 0.3, 0.5, 0.7]$ and $s_{int} \in [0.0, 0.1, 0.2, 0.3]$. We observe that the smaller the area of cropped images, the higher the performance. It suggests that local image patches that differ significantly from the original images provide more diverse input patterns for perturbation optimization and contribute to targeted transferability. Besides, when $s_l = 0.1$ and $s_{int} = 0.1$, the optimal result is reached. However, the area relative to the original image may fluctuate within $[0.1, 0.2]$. To keep it stable, we use the parameters $s = (0.1, 0.0)$ of the sub-optimal result to conduct subsequent experiments. Figure 3(b) shows the results of performing attacks on different layers and λ . Extracting features from layer 3 is better than other layers. This is consistent with the observations in (Wei et al. 2022b). For the weighted parameter λ , we set $\lambda \in [0.4, 0.6, 0.8, 1.0]$. When $\lambda = 0.4$, LI achieves the best result.

Conclusion

In this paper, we provide new insight into targeted transferability, that is targeted transferable perturbations tend to be universal to images. Based on this observation, we propose the Locality of Images (LI) attack, which optimizes perturbations on both global and local images, and aligns intermediate features between them. Through incorporating local structures with global structures, LI can tune the suitability of crafted perturbations and boost targeted transferability. Besides, the proposed LI can easily be combined with existing transfer-based attack methods. We conduct extensive experiments to show that LI can improve targeted transferability regardless of the single-model attack or ensemble-based attack. The combination of the proposed LI and DTMI consistently outperforms the baseline attacks by 12%. Our best targeted attack, DTMI-Logit-LI can achieve a 69.6% TASR on average in the ensemble-based scenario. The results demonstrate that adversarial perturbations with high universality can be more transferable even across wide architectural gaps between models, posing threats to the real-

world applications of models. In the future, we will solve the problem that the value of the logit loss increases infinitely by an adaptive weighted parameter, and construct importance-aware features to further boost targeted transferability.

References

- Biggio, B.; Corona, I.; Maiorca, D.; Nelson, B.; Srndic, N.; Laskov, P.; Giacinto, G.; and Roli, F. 2013. Evasion Attacks against Machine Learning at Test Time. In *ECML/PKDD*.
- Deng, J.; Dong, W.; Socher, R.; Li, L.-J.; Li, K.; and Fei-Fei, L. 2009. ImageNet: A large-scale hierarchical image database. *2009 IEEE Conference on Computer Vision and Pattern Recognition*, 248–255.
- Dong, Y.; Liao, F.; Pang, T.; Su, H.; Zhu, J.; Hu, X.; and Li, J. 2018. Boosting adversarial attacks with momentum. In *Proceedings of the IEEE conference on computer vision and pattern recognition*, 9185–9193.
- Dong, Y.; Pang, T.; Su, H.; and Zhu, J. 2019. Evading Defenses to Transferable Adversarial Examples by Translation-Invariant Attacks. *2019 IEEE/CVF Conference on Computer Vision and Pattern Recognition (CVPR)*, 4307–4316.
- Goodfellow, I. J.; Shlens, J.; and Szegedy, C. 2014. Explaining and harnessing adversarial examples. *arXiv preprint arXiv:1412.6572*.
- He, K.; Zhang, X.; Ren, S.; and Sun, J. 2016. Deep Residual Learning for Image Recognition. *2016 IEEE Conference on Computer Vision and Pattern Recognition (CVPR)*, 770–778.
- Huang, G.; Liu, Z.; and Weinberger, K. Q. 2017. Densely Connected Convolutional Networks. *2017 IEEE Conference on Computer Vision and Pattern Recognition (CVPR)*, 2261–2269.
- Inkawhich, N.; Liang, K.; Wang, B.; Inkawhich, M.; Carin, L.; and Chen, Y. 2020a. Perturbing across the feature hierarchy to improve standard and strict blackbox attack transferability. *Advances in Neural Information Processing Systems*, 33: 20791–20801.
- Inkawhich, N.; Liang, K. J.; Carin, L.; and Chen, Y. 2020b. Transferable perturbations of deep feature distributions. *arXiv preprint arXiv:2004.12519*.
- Inkawhich, N.; Wen, W.; Li, H. H.; and Chen, Y. 2019. Feature space perturbations yield more transferable adversarial examples. In *Proceedings of the IEEE/CVF Conference on Computer Vision and Pattern Recognition*, 7066–7074.
- Kurakin, A.; Goodfellow, I. J.; and Bengio, S. 2017. Adversarial Machine Learning at Scale. *ArXiv*, abs/1611.01236.
- Kurakin, A.; Goodfellow, I. J.; and Bengio, S. 2018. Adversarial examples in the physical world. In *Artificial intelligence safety and security*, 99–112. Chapman and Hall/CRC.
- Li, M.; Deng, C.; Li, T.; Yan, J.; Gao, X.; and Huang, H. 2020. Towards Transferable Targeted Attack. *2020 IEEE/CVF Conference on Computer Vision and Pattern Recognition (CVPR)*, 638–646.
- Lin, J.; Song, C.; He, K.; Wang, L.; and Hopcroft, J. E. 2020. Nesterov Accelerated Gradient and Scale Invariance for Adversarial Attacks. *arXiv: Learning*.
- Liu, Y.; Chen, X.; Liu, C.; and Song, D. 2017. Delving into Transferable Adversarial Examples and Black-box Attacks. In *International Conference on Learning Representations*.
- Moosavi-Dezfooli, S.-M.; Fawzi, A.; Fawzi, O.; and Frossard, P. 2017. Universal Adversarial Perturbations. *2017 IEEE Conference on Computer Vision and Pattern Recognition (CVPR)*, 86–94.
- Naseer, M.; Khan, S.; Hayat, M.; Khan, F. S.; and Porikli, F. 2021. On generating transferable targeted perturbations. In *Proceedings of the IEEE/CVF International Conference on Computer Vision*, 7708–7717.
- Selvaraju, R. R.; Das, A.; Vedantam, R.; Cogswell, M.; Parikh, D.; and Batra, D. 2017. Grad-CAM: Visual Explanations from Deep Networks via Gradient-Based Localization. *International Journal of Computer Vision*, 128: 336–359.
- Simonyan, K.; and Zisserman, A. 2015. Very Deep Convolutional Networks for Large-Scale Image Recognition. *CoRR*, abs/1409.1556.
- Szegedy, C.; Vanhoucke, V.; Ioffe, S.; Shlens, J.; and Wojna, Z. 2016. Rethinking the Inception Architecture for Computer Vision. *2016 IEEE Conference on Computer Vision and Pattern Recognition (CVPR)*, 2818–2826.
- Wang, X.; and He, K. 2021. Enhancing the Transferability of Adversarial Attacks through Variance Tuning. *2021 IEEE/CVF Conference on Computer Vision and Pattern Recognition (CVPR)*, 1924–1933.
- Wang, Z.; Guo, H.; Zhang, Z.; Liu, W.; Qin, Z.; and Ren, K. 2021. Feature Importance-aware Transferable Adversarial Attacks. *2021 IEEE/CVF International Conference on Computer Vision (ICCV)*, 7619–7628.
- Wei, Z.; Chen, J.; Wu, Z.; and Jiang, Y.-G. 2022a. Boosting the Transferability of Video Adversarial Examples via Temporal Translation. In *Proceedings of the AAAI Conference on Artificial Intelligence*, volume 36, 2659–2667.
- Wei, Z.; Chen, J.; Wu, Z.; and Jiang, Y.-G. 2022b. Cross-Modal Transferable Adversarial Attacks from Images to Videos. In *Proceedings of the IEEE/CVF Conference on Computer Vision and Pattern Recognition*, 15064–15073.
- Wu, D.; Wang, Y.; Xia, S.; Bailey, J.; and Ma, X. 2020a. Skip Connections Matter: On the Transferability of Adversarial Examples Generated with ResNets. *ArXiv*, abs/2002.05990.
- Wu, W.; Su, Y.; Chen, X.; Zhao, S.; King, I.; Lyu, M. R.; and Tai, Y.-W. 2020b. Boosting the Transferability of Adversarial Samples via Attention. *2020 IEEE/CVF Conference on Computer Vision and Pattern Recognition (CVPR)*, 1158–1167.
- Xie, C.; Zhang, Z.; Zhou, Y.; Bai, S.; Wang, J.; Ren, Z.; and Yuille, A. L. 2019. Improving transferability of adversarial examples with input diversity. In *Proceedings of the IEEE/CVF Conference on Computer Vision and Pattern Recognition*, 2730–2739.
- Zhang, C.; Benz, P.; Imtiaz, T.; and Kweon, I. S. 2020. Understanding Adversarial Examples From the Mutual Influence of Images and Perturbations. *2020 IEEE/CVF Conference on Computer Vision and Pattern Recognition (CVPR)*, 14509–14518.

Zhao, Z.; Liu, Z.; and Larson, M. 2021. On success and simplicity: A second look at transferable targeted attacks. *Advances in Neural Information Processing Systems*, 34: 6115–6128.